Ozone direct oxidation kinetics of Cationic Red X-GRL in aqueous solution

Weirong Zhao *, Zhongbiao Wu, Dahui Wang

Department of Environmental Engineering, Zhejiang University, Hangzhou 310027, China

Abstract

This study characterizes the ozonation of the azo dye Cationic Red X-GRL in the presence of TBA (*tert*-butyl alcohol), a scavenger of hydroxyl radical, in a bubble column reactor. Effects of oxygen flow rate, temperature, initial dye concentration, and pH were investigated through a series of batch tests. Generally, enhancing oxygen flow rate enhanced the removal of dye. However, there was a minimum removal of dye at temperature 298 K. Increasing or decreasing temperature enhanced the degradation of dye. Increasing the initial dye concentration decreased the removal of dye while the ozonation rate increased. The rate constants and the kinetic regime of the reaction between ozone and dye were obtained by fitting the experimental data to a kinetics model based on a second order overall reaction, first order with respect to both ozone and dye. The Hatta numbers of the reactions were between 0.039 and 0.083, which indicated that the reaction occurred in the liquid bulk. The direct oxidation rate constant k_D was correlated with temperature by a modified Arrhenius Equation with an activation energy E_a of 15.538 kJ mol^{-1}.
© 2006 Elsevier B.V. All rights reserved.

Keywords: Ozonation; Kinetics; Mass transfer; Azo dye; Water treatment

1. Introduction

The treatment of textile wastewater is an environmental concern since the associated color of textile wastewater is quite noticeable to the public, and some dyes in textile wastewater may have carcinogenic and/or teratogenic effects on public health. A lot of researches have demonstrated that conventional treatment processes cannot efficiently remove dyes from textile wastewater, because of dyes' stability to light, and biological degradation [1]. Ozonation, an easy-operated oxidation technology, is very effective in treating wastewaters containing recalcitrant compounds [2]. Ozone and hydroxyl radicals ($^\bullet$OH) generated by ozone in the aqueous solution are able to break aromatic rings of dyes. Typically, ozonation rarely leads to the complete mineralization but partial oxidation of dyes to organic acids, aldehydes, and ketones [3]. During the ozonation process, dyes lose their color due to the oxidative cleavage of the chromophores. The cleavage of carbon–carbon double bonds and other functional groups with high electron densities will shift the absorption spectra of the molecule out of the visible region [4].

The role of ozonation in treating several organic substances has been examined by different researchers [5–9]. However, most of these works paid little attention to the interaction between gas–liquid mass transfer and chemical reaction, and there are only a few kinetic data available for those processes [9–12].

Cationic Red X-GRL, an azo dye, was selected as the model pollutant for this study because it is not biodegradable by the conventional activated sludge process [13], and it is widely used in the textile, color solvent, ink, paint, varnish, paper, and plastic industries.

tert-Butyl alcohol used in the present work is practically inert toward ozone [$k_D \leq 3 \times 10^{-3}$ M^{-1} s^{-1}], it acts as an hydroxyl radical scavenger [$k_R = 6 \times 10^8$ M^{-1} s^{-1}] and inhibits the chain reaction between $^\bullet$OH and dye [14]. The mass transfer and ozone direct oxidation of Cationic Red X-GRL in aqueous solutions was investigated simultaneously to obtain the kinetic parameters: reaction orders and rate constants. The enhancement factor and the kinetic regime of absorption were also determined by fitting the experimental data with a film mass transfer model.

---

* Corresponding author. Tel.: +86 571 8795 1239; fax: +86 571 8795 2771.
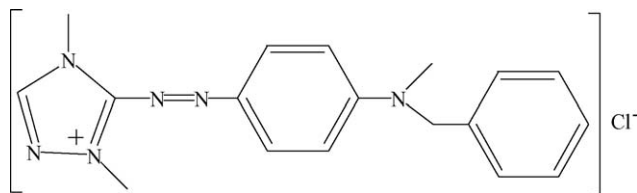*E-mail address:* weirong@mail.hz.zj.cn (W. Zhao).

Fig. 1. Structural formula of Cationic Red X-GRL.

2. Material and methods

2.1. Reagents

The commercial azo dye Cationic Red X-GRL (Xinya Silk Weaving Mill, Wujiang, Jiangsu, China), 5-[4-(benzyl-methyl-amino)-phenylazo]-1,4-dimethyl-4H-[1,2,4]triazol-1-ium chloride, was purified by the methanol recrystallization method before used. As shown in Fig. 1, its cation part connects with a chloride ion by ionic bond. The molecular weight of the dye is $356.84\,\mathrm{g\,mol^{-1}}$, and the dye has a maximum UV–vis absorbance at 530 nm. Indigo trisulfonate was purchased from Fluka Chemical, USA.

Ionic strength of 5.0 M concentrated phosphate buffer solutions was prepared by mixing a calculated amount of sodium hydroxide solution and a phosphoric acid solution.

2.2. Apparatus

A schematic of the experimental set-up for ozonation is depicted in Fig. 2. Ozone was produced from dry and pure oxygen by a CHYF-3A model ozone generator (Rongxing Elec. Co. Ltd., China) that is able to generate a maximum of $3\,\mathrm{g\,ozone\,h^{-1}}$. The 3.5 L Pyrex glass bubble column reactor was equipped with a few inlets for bubbling the feed gas, sampling, venting, and measuring temperature. Excess ozone was passed into two gas absorption bottles containing 2% KI solution. All tubes from the ozone generator to the reactor and the gas absorption bottles were made of Neoprene and the fittings were made of Teflon. The experiments were carried out in a thermostatic bath to keep the temperature at the desired value $\pm 0.5\,^{\circ}\mathrm{C}$.

2.3. Ozonation of Cationic Red X-GRL

Dye ozonation experiments were conducted in the bubble column reactor containing 3.5 L dye solutions. The dye solutions
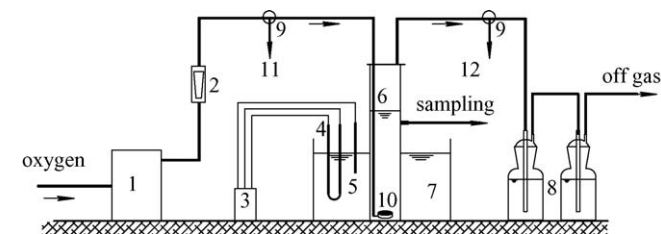

Fig. 2. Schematic of the experimental set-up: (1) ozone generator; (2) rotameter; (3) temperature controller; (4) electrical heater; (5) thermocouple; (6) bubble column reactor; (7) thermostatic bath; (8) absorption bottle; (9) three-way valve; (10) porous plate; (11) to input ozone gas detection; (12) to off gas detection.

were buffered by phosphate buffer solutions to reach a desired pH. The ionic strength of the dye solutions was controlled at 0.1 M. The concentration of *tert*-butyl alcohol in the dye solutions was maintained at 50 mM to avoid the oxidation of dye by hydroxyl radicals. Before the reaction, the ozone concentration in ozone–oxygen mixture stream from ozone generator was determined. Once the ozonation process started, samples were taken from reactor periodically to analyze the concentration of Cationic Red X-GRL and dissolved ozone.

2.4. Reaction ratio between ozone and Cationic Red X-GRL

The reaction stoichiometric ratio z between ozone and Cationic Red X-GRL was determined as follows. Excess Cationic Red X-GRL (high concentration of dye and limited ozone) and ozone solutions were mixed quickly to assure the complete consumption of ozone at an instantaneous rate. 50 mM *tert*-butyl alcohol was maintained in the aqueous solutions to avoid the side reaction between dye and hydroxyl radicals. The ozone solutions were prepared by bubbling an ozone–oxygen mixture stream into high purity water (0.1 µS conductivity) ca. 30 min till saturation. The reaction ratio z between ozone and Cationic Red X-GRL is calculated using Eq. (1):

$$z = \frac{C_{A,0}}{C_{B,0} - C_B} \tag{1}$$

where $C_{A,0}$ is the initial dissolved ozone concentration, $C_{B,0}$ the initial dye concentration, and C_B is the remaining dye concentration in the solution.

2.5. Analytical methods

TU1800PC UV–vis spectrophotometer (Pgenral Analytical Instrument Co. Ltd., Beijing, China) was used to determine the concentrations of Cationic Red X-GRL.

The pH value was measured by pHS-25 (Rex Analytical Instrument Co. Ltd., Shanghai, China). The input and off gas mass concentration of ozone was determined by iodometrical method [15]. The partial pressure of the ozone gas P_A was determined by the difference of input and off gas mass concentration of ozone. The concentration of ozone in solutions was also measured colorimetrically by the Indigo method [16].

3. Results and discussion

3.1. Determination of k_L and a

In order to investigate the mass transfer process of dye oxidation by ozone, preliminary experiments [17] were conducted to determine the mass transfer coefficient k_L (ozone to liquid phase) and the interfacial area a. In these experiments, pure carbon dioxide was bubbled into sodium carbonate–bicarbonate (0.5–0.5 M) buffer solutions with sodium arsenite as catalyst. The kinetics of this absorption reaction is in the pseudo-first order kinetic regime. The mass transfer coefficient k_L of CO_2 adsorption and the interfacial area a were obtained using the "Danckwerts's plot method" [12]. The mass transfer coefficients

Table 1
Interfacial areas and mass transfer coefficient values

T (K)	Q_g (L h^{-1})	$k_L \times 10^5$ (m s^{-1})	a (m^{-1})	$k_L a \times 10^3$ (s^{-1})
288	100	8.19	110.2	9.02
293	100	9.83	107.3	10.55
298	100	12.17	105.1	12.79
303	100	13.52	100.5	13.59
308	100	14.96	96.6	14.45
298	70	10.04	72.3	7.26
298	40	8.25	60.8	5.01

of ozone to liquid phase were then determined through Eq. (2) [12]:

$$k_L = k'_L \left(\frac{D_A}{D_C} \right)^{1/2} \quad (2)$$

where k_L is the mass transfer coefficient of ozone to liquid phase, k'_L the mass transfer coefficient of carbon dioxide absorption into sodium carbonate–bicarbonate solution, D_A the diffusivity of ozone in liquid phase obtained from Matrozov et al. [18] and D_C is the diffusivity of carbon dioxide in liquid phase.

The k_L and a values for various temperatures T and oxygen flow rates Q_g are summarized in Table 1.

3.2. Determination of stoichiometric ratio

Fig. 3 shows that a stoichiometric ratio z of 4 between ozone and dye was achieved at various pHs (3.15, 5.75, 8.14, and 9.24). It can be observed in Fig. 3 that z takes a high value and decreases, as the initial dye/ozone ratio increases until it reaches a constant value.

There are two different reaction pathways between ozone and organic compounds [3]: direct attack of ozone and free radical attack of hydroxyl radical. Fig. 3 shows that almost same stoichiometric ratios were achieved at different pHs, which indicates that the reaction is mainly due to ozone direct attack, while the
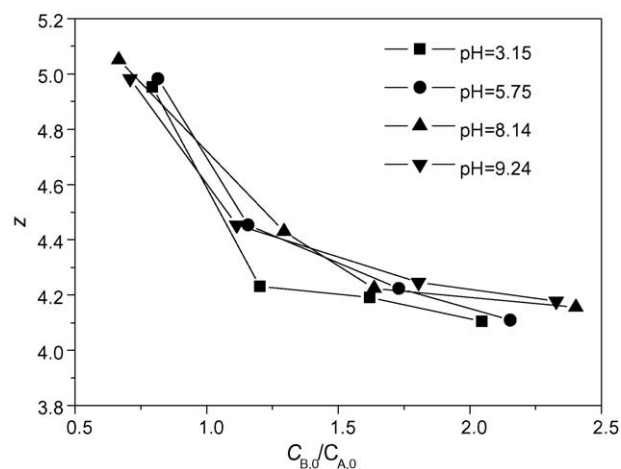

Fig. 3. Determination of the stoichiometric ratios for the ozone–dye reactions.

formation of radicals by ozone decomposition, and hence radical attack, is almost negligible. This is due to the fact that the *tert*-butyl alcohol used in the buffer solutions are scavengers of free radicals [3].

The fact that 1 mol dye consumed 4 moles ozone can be explained by a simplified degradation mechanism of Cationic Red X-GRL by ozone [13] as depicted in Fig. 4. During ozonation, the first ozone molecule was consumed in the cleavage of dye (reaction (1)) to nitrite ion, compound D_1, and S_4. The second ozone molecule was consumed in the oxidation of nitrite ion to nitrate ion (direct reaction rate k_D of reaction (3) is 3.7×10^5 M^{-1} s^{-1} [19]). The third ozone molecule was consumed in the decomposition of compound S_4 to compound D_2 and D_3 (reaction (4)). The fourth ozone molecule was consumed in the cleavage of heterocyclic ring of compound D_2 to compound D_4 (reaction (5)). It is noteworthy that the ozone consumption rates of reactions (2), (6), and (7) were negligible because aldehydes or ketones are very recalcitrated to be oxidized by ozone (direct reaction rate k_D of reaction (2) is 2.5 M^{-1} s^{-1} [20]).
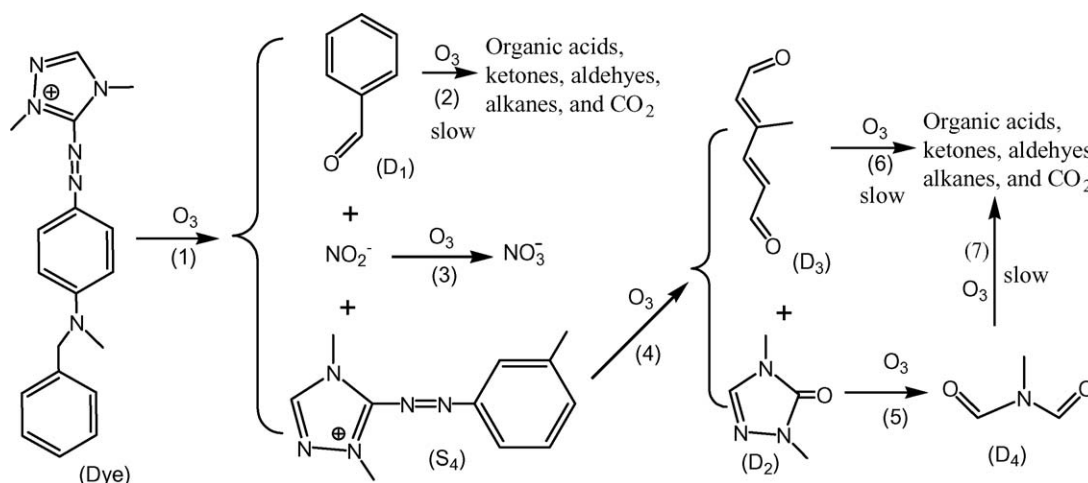

Fig. 4. Simplified degradation pathways of Cationic Red X-GRL. D_1 = benzaldehyde; D_2 = 2,4-dimethyl-2,4-dihydro-[1,2,4] triazol-3-one; D_3 = 3-methyl-hexa-2,4-dienedial; D_4 = N-formyl-N-methyl-formamide; S_4 = ozonation intermediate.
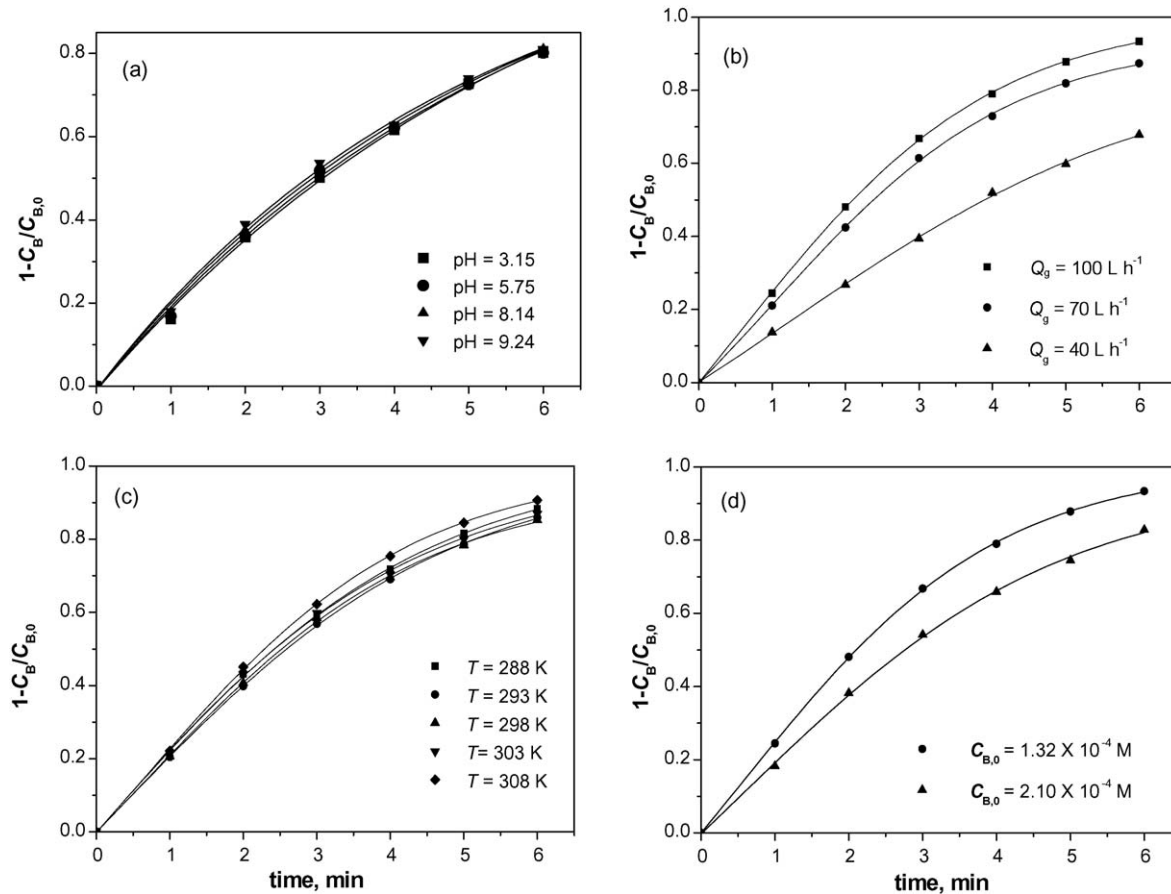
Fig. 5. Effect of process variables on conversion of dye. (a) Effect of pHs. Runs 5–8 (Table 2). (b) Effect of oxygen flow rates. Runs 3, 9–10 (Table 2). (c) Effect of temperatures. Runs 2, 11–14 (Table 2). (d) Effect of initial concentrations of dye. Runs 2, 6 (Table 2).

3.3. Influence of reaction variables

Fig. 5 shows the conversion of dye with time for a set of experiments carried out under different oxygen flow rate, initial dye concentration $C_{B,0}$, temperature, and pH. The experimental parameters and results are listed in Table 2.

As mentioned before, the dye degradation caused by radical attack is negligible in this study. Therefore, the increase of pH did not cause obvious enhanced removal of dye as depicted in Fig. 5a.

However, the oxygen flow rates have a positive effect on the dye degradation. As shown in Fig. 5b, at 6 min the con-

Table 2
Experimental conditions and calculation results

Run	T (K)	pH	Q_g (L h^{-1})	P_A (kPa)	$C_A^{*\dagger} \times 10^4$ (M)	$C_{B,0} \times 10^4$ (M)	E	k_D (M^{-1} s^{-1})	$Ha \times 10^3$
1	298	3.15	100	1.74	1.40	1.28	1.08	203	52
2	298	5.75	100	1.71	1.30	1.32	1.18	206	53
3	298	8.14	100	1.77	1.22	1.27	1.45	203	52
4	298	9.24	100	1.75	1.18	1.49	1.61	202	56
5	298	3.15	100	1.75	1.40	2.09	1.37	203	67
6	298	5.75	100	1.70	1.26	2.10	1.59	209	68
7	298	8.14	100	1.68	1.17	2.13	1.92	198	66
8	298	9.24	100	1.76	1.19	2.21	1.95	209	69
9	298	8.14	70	1.78	1.22	1.30	2.52	199	63
10	298	8.14	40	1.74	1.22	1.46	2.42	205	83
11	288	5.75	100	1.82	1.67	1.40	1.40	161	63
12	293	5.75	100	1.80	1.47	1.44	1.29	192	60
13	303	5.75	100	1.77	1.16	1.43	1.36	225	53
14	308	5.75	100	1.76	1.04	1.44	1.60	252	56

† The equilibrium concentration of ozone in water C_A^* was deduced by Henry's law; while the Henry's law constants of ozone as a function of pH and temperature were obtained from Sotelo et al. [21].
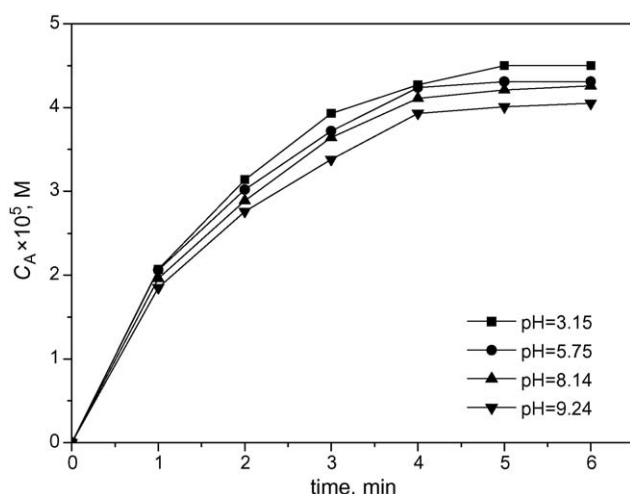
Fig. 6. Aqueous ozone concentration accumulation with reaction time. Runs 1–4 (Table 2).

versions of dye were 93, 87, and 67% for the oxygen flow rates of 100, 70, and 40 L h^{-1}, respectively. As shown in Table 1, at 298 K the volumetric mass transfer coefficient k_La of bubble column reactor increased from 5.01×10^{-3} s^{-1} at the oxygen flow rate of 40 L h^{-1} to 7.26×10^{-3} s^{-1} at the oxygen flow rate of 70 L h^{-1}, and 12.79×10^{-3} s^{-1} at the oxygen flow rate of 100 L h^{-1}, respectively. It is worthy to mention that the partial pressures of the ozone gas P_A were quite stable in our study as shown in Table 2 (Runs 3, 9–10). In addition, the ozone mass transfer rate was proportional to the volumetric mass transfer coefficient k_La of the bubble column reactor.

The effect of temperature on the conversion of dye is shown in Fig. 5c. At 6 min, the conversions of dye were 88, 86, 85, 87, and 91% for reaction temperatures of 288, 293, 298, 303, and 308 K, respectively. A minimum conversion of dye was observed at temperature 298 K. This is because if temperature increased the reaction rate constant and the volumetric mass transfer coefficient k_La of bubble column reactor increased (Table 1), however the ozone equilibrium concentration [21] decreased correspondingly.

Fig. 5d shows the evolution of the conversion of dye with time for experiments carried out at different initial dye concentration. At a given time, an increase of initial dye concentration led to a decreased conversion of dye though the ozonation rate increased. Thus, at 6 min, 96% dye conversion was reached if the initial dye concentration was 1.32×10^{-4} M, while ca. 83% conversion was reached if the initial dye concentration was 2.10×10^{-4} M. However, initial dye removal rates were 4.60×10^{-7} and 6.15×10^{-7} M s^{-1} for initial dye concentrations of 1.32×10^{-4} and 2.10×10^{-4} M, respectively.

It is noteworthy that the aqueous ozone concentration accumulates with reaction time, as shown in Fig. 6. This accumulation can be explained by the slow reaction kinetics between dye and ozone, which will be confirmed afterwards.

3.4. Kinetic study

According to the film theory, when the absorption of a gas into a liquid solution is accompanied by an irreversible chemical reaction with another compound dissolved in the liquid, this reaction can occur in the liquid bulk (slow kinetic regime), in the liquid film (fast kinetic regime), or in both liquid film and the diffusion film (moderate fast kinetic regime), depending on the operating and kinetic variables [22].

The gas absorption rate with slow kinetic regime reaction can be described by Eq. (3):

$$N_A a = k_L a C_A^* E \qquad (3)$$

where $N_A a$ is the ozone absorption rate of liquid phase, $k_L a$ the volumetric mass transfer coefficient of bubble column reactor, C_A^* the equilibrium concentration of ozone in water and E is the enhancement factor defined as the ratio of the rate of absorption in the presence of a chemical reaction to the maximum rate of pure physical absorption.

The ozone absorption rate is the combination of its consumption rate by dye and its accumulation rate in liquid phase:

$$N_A a = -\frac{z \, dC_B}{dt} + \frac{dC_A}{dt} \qquad (4)$$

where z is the reaction ratio between ozone and Cationic Red X-GRL, C_B the concentration of dye in liquid phase, C_A the concentration of ozone in liquid phase and t is the reaction time. In all the experiments, the values of dC_A/dt were always found to be less than 6% of the values of $-z \, dC_B/dt$. In order to simplify the mathematical model, the term of dC_A/dt is ignored in the following discussion. Thus

$$N_A a = -\frac{z \, dC_B}{dt} \qquad (5)$$

Combining Eqs. (3) and (5) together, the enhancement factor E can be deduced as following equation:

$$E = -\frac{z \, dC_B}{k_L a C_A^* \, dt} \qquad (6)$$

The values of dC_B/dt can be determined through fitting the experimental data (C_B, t) to a polynomial expression by least square regression analysis. Table 2 shows the E values obtained at $t = 0$. As shown in Table 2, the E values were less than 3, indicating that the reaction in the liquid bulk was slow [22]. Assuming that the degradation rate of dye follows first order kinetic with respect to both ozone and dye, we get:

$$-\frac{dC_B}{dt} = k_D C_B C_A \qquad (7)$$

where k_D is the ozone direct oxidation rate constant.

Then,

$$-\ln\left(\frac{C_B}{C_{B,0}}\right) = k_D \int_0^t C_A \, dt \qquad (8)$$

k_D can be calculated by linear regression analysis with experimental data given in Table 2. Fig. 7 shows the calculation of k_D which were strongly influenced by temperature. However, k_D was not influenced by pH, oxygen flow rate, and initial dye concentration as shown in Table 2.
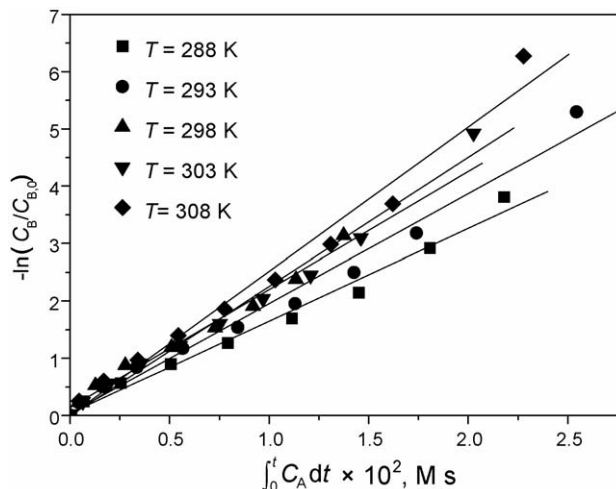
Fig. 7. Determination of k_D with temperature. Runs 2, 11–14 (Table 2).

Through Arrhenius Equation:

$$k_D = k_0 \exp\left(\frac{-E_a}{RT}\right) \qquad (9)$$

activation energy E_a of the ozonation of Cationic Red X-GRL can be calculated. Fig. 8 depicts the Arrhenius plot of the natural logarithm of the k_D versus $1/T$ for the ozonation of Cationic Red X-GRL. The activation energy E_a was calculated to be 15.538 kJ mol^{-1} and $k_0 = 1.0881 \times 10^5$ M^{-1} s^{-1}.

In order to determine that the reaction between ozone and Cationic Red X-GRL occurred in the liquid bulk or in the liquid film or in both, dimensionless Hatta number Ha was calculated for all experiments. Hatta number allows ascertaining the type of kinetic regime [22]: for low values of Ha, between 0.02 and 0.3, indicate that the reaction occurs in the slow regime; for values higher than 3, in the fast regime; and for values between 0.3 and 3, in the moderately fast regime. For a second order irreversible reaction, the Hatta number takes the form [22]:

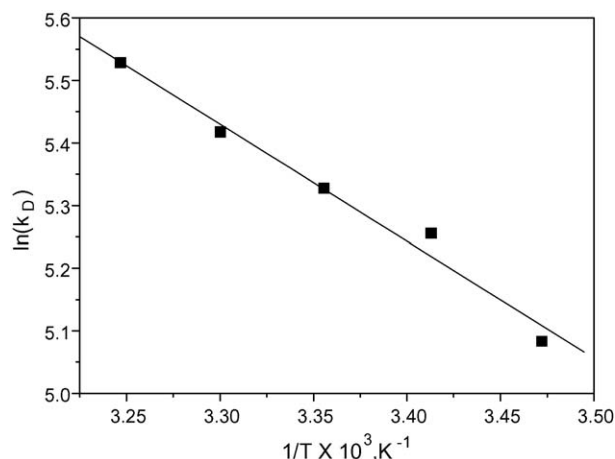$$Ha = \left(\frac{D_A k C_B}{k_L^2}\right)^{1/2} \qquad (10)$$

Fig. 8. Plot of $\ln(k_D)$ vs. $1/T$.

Table 2 shows that the calculated Ha values for the initial period of reaction were always between 0.052 and 0.083. Thus, the reaction between ozone and Cationic Red X-GRL is in slow kinetics regime and occurred in the bulk phase for all performed experiments.

4. Conclusion

The results obtained in this work indicate that the absorption of ozone into aqueous solutions of the Cationic Red X-GRL was accompanied by an irreversible second order reaction. The reaction between ozone and Cationic Red X-GRL occurred in the liquid bulk, corresponding to the slow kinetic regime. The influence of operating variables like oxygen flow rate, initial dye concentration, temperature, and pH was also established. The kinetic rate constants were correlated with Arrhenius Equation by the expression:

$$k_D = k_0 \exp\left(\frac{-E_a}{RT}\right) = 108,810 \exp\left(\frac{-15,538}{RT}\right) \ (\text{M}^{-1}\,\text{s}^{-1})$$
$$(11)$$

References

[1] A.M. Talarposhti, T. Donnelly, G.K. Anderson, Colour removal from a simulated dye wastewater using a two-phase anaerobic packed bed reactor, Water Res. 35 (2001) 425–432.

[2] W. Chu, M.H. Ching, Modeling the ozonation of 2,4-dichlorophoxyacetic acid through a kinetic approach, Water Res. 37 (2003) 39–46.

[3] J. Staehelin, J. Hoigné, Decomposition of ozone in water in the presence of organic solutes acting as promoters and inhibitors of radical chain reactions, Environ. Sci. Technol. 19 (1985) 1206–1213.

[4] H.Y. Shu, C.R. Huang, M.C. Chang, Decolorization of mono-azo dyes in wastewater by advanced oxidation process: a case study of acid red 1 and acid yellow 23, Chemosphere 29 (1994) 2597–2607.

[5] H.Y. Shu, M.C. Chang, Pre-ozonation coupled with UV/H$_2$O$_2$ process for the decolorization and mineralization of cotton dyeing effluent and synthesized C. I. Direct Black 22 wastewater, J. Hazard. Mater. B 121 (2005) 127–133.

[6] H.Y. Shu, M.C. Chang, Decolorization effects of six azo dyes by O$_3$, UV/O$_3$ and UV/H$_2$O$_2$ processes, Dyes Pigments 65 (2005) 25–31.

[7] H. Selcuk, Decolorization and detoxification of textile wastewater by ozonation and coagulation processes, Dyes Pigments 64 (2005) 217–222.

[8] M. Neamtu, A. Yediler, I. Siminiceanua, M. Macoveanua, A. Kettrup, Decolorization of disperse red 354 azo dye in water by several oxidation processes-a comparative study, Dyes Pigments 60 (2004) 61–68.

[9] Y.H. Chen, C.Y. Chang, S.F. Huang, N.C. Shang, C.Y. Chiu, Y.H. Yu, P.C. Chiang, J.L. Shie, C.S. Chiou, Decomposition of 2-naphthalenesulfonate in electroplating solution by ozonation with UV radiation, J. Hazard. Mater. B 118 (2005) 177–183.

[10] E. Oguz, B. Keskinler, C. Çelik, Z. Çelik, Determination of the optimum conditions in the removal of Bomaplex Red CR-L dye from the textile wastewater using O$_3$, H$_2$O$_2$, HCO$_3$ and PAC, J. Hazard. Mater. B 131 (2006) 66–72.

[11] F.J. Benitez, J. Beltrán-Heredia, J.A. Peres, J.R. Dominguez, Kinetics of *p*-hydroxybenzoic acid photodecomposition and ozonation in a batch reactor, J. Hazard. Mater. B 73 (2000) 161–178.

[12] J. Beltrán-Heredia, J. Torregrosa, J.R. Dominguez, J.A. Peres, Kinetics of the reaction between ozone and phenolic acids present in argo-industrial wastwaters, Water Res. 35 (2001) 1077–1085.

[13] W.R. Zhao, H.X. Shi, D.H. Wang, Ozonation of Cationic Red X-GRL in aqueous solution: degradation and mechanism, Chemosphere 57 (2004) 1189–1199.

[14] P. Neta, R.E. Huie, A.B. Ross, Rate constants for reactions of inorganic radicals in aqueous solutions, J. Phys. Chem. Ref. Data 17 (1988) 1027–1284.

[15] G.R. Peyton, W.H. Glaze, Destruction of pollutants in water with ozone in combination with ultraviolet radiation. 3. Photolysis of aqueous ozone, Environ. Sci. Technol. 22 (1988) 183–189.

[16] H. Bader, J. Hoigne, Determination of ozone in water by the indigo method, Water Res. 15 (1981) 449–456.

[17] W.R. Zhao, H.X. Shi, D.H. Wang, Modeling of mass transfer characteristic of bubble column reactor in the presence of surfactant, J. Zhejiang Univ. Sci. 5 (2004) 714–720.

[18] V. Matrozov, S. Kachtunov, B. Tregunov, A. Stepanov, Experimental determination of the molecular diffusion coefficient of ozone in water, Zh. Prikl. Khim. 49 (1976) 1070–1073.

[19] J. Hoigné, H. Bader, W.R. Haag, J. Staehelin, Rate constants of reactions of ozone with organic and inorganic compounds in water. III. Inorganic compounds and radicals, Water Res. 19 (1985) 993–1004.

[20] J. Hoigné, H. Bader, Rate constants of reactions of ozone with organic and inorganic compounds in water. I. Non-dissociated organic compounds, Water Res. 17 (1983) 173–183.

[21] J.L. Sotelo, F.J. Beltrán, F.J. Benitez, J. Beltrán-Heredia, Henry's law constant for the ozone–water system, Water Res. 23 (1989) 1239–1246.

[22] J.C. Charpentier, Mass-transfer rates in gas–liquid absorbers and reactors, in: T.B. Drew, G.R. Cokelet, H.W. Hoopes Jr., T. Vermeulen (Eds.), Advances in Chemical Engineering, vol. 11, Academic Press, New York, 1981, pp. 3–133.